

Study of Micro X-ray Fluorescence Spectrometry as a method for in-vivo phenotyping of *Arabidopsis thaliana*

W. Tramel†, U. E. A. Fittschen†, H. H. Kunz*, I. M. B. Tyssebotn*, A. Fittschen†

†Department of Chemistry, Washington State University, Pullman WA, 99164, USA

*Plant Physiology, School of Biological Science, Washington State University, Pullman WA, 99164, USA

Introduction

With genetic modification comes the challenge of characterizing the phenotype of the organism. Phenotyping studies how the genome of an organism is expressed, such as hair or eye color. The genetic alteration being explored by the Washington State University School of Biological Sciences Plant Physiology lab involve knocking out a protein that is believed to be involved in ion transport within the leaf cells to determine how the protein is involved. This is accomplished by analysis of the differences in potassium and calcium (K and Ca) ion gradients in the leaves of the two plant types.

To accurately compare gradients between plant types, the analysis must not disturb the natural elemental concentrations or elemental distributions within the leaf. With the micro-XRF method, the sample is exposed to an x-ray source and the resulting fluorescence spectrum is recorded. The spectra are compiled as individual pixels to form a composite image of the elemental concentrations (Fig. 1 and 2).

Little to no sample preparation is required and limited exposure of the plant to the incident x-rays was shown to be not harmful to the plant [Fittschen et al XRS 2017]. Since μ -XRF only requires that the sample be in the correct position between the x-ray source and the detector living plants can be analyzed in vivo. This study aims to explore the capability of the custom built micro-XRF for phenotyping by micro-ionome analysis differentiating between plant organs like veins and mesophyll.

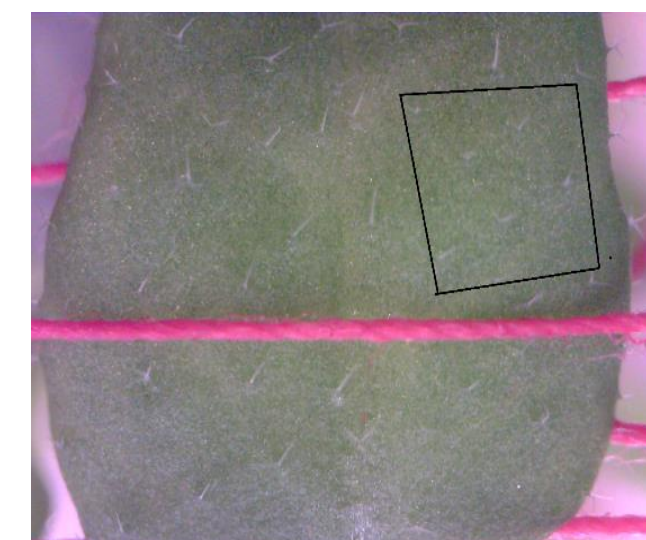


Figure 1: Optical image of the leaf surface with box showing the scanned area.

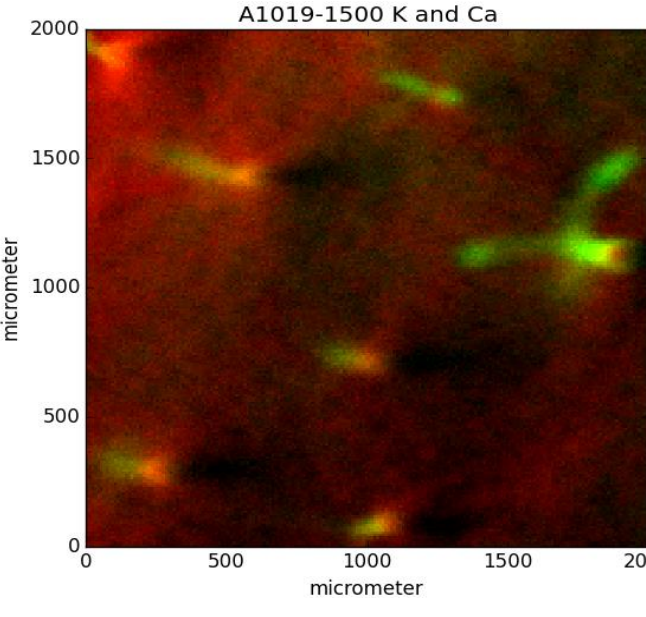


Figure 2: False color RGB elemental map of relative K (red) and Ca (green) concentrations.

XRF and Micro-XRF

X-Ray Fluorescence (XRF)

Though the principles of XRF are similar to those of optical fluorescence both being non-invasive, in contrast XRF is an atomic spectrometry tool rather than molecular spectrometry. XRF uses x-rays to eject a core electron from its shell. A higher energy electron must fall to fill the vacancy, emitting an X-ray of characteristic energy as it falls. Specific transition energies are described with K, L, and M for the shell that the electron to and α or β depending on the shell that the electron fell from. The energy associated with each transition is unique for each element regardless of the chemical environment. The unique energy of the observed fluorescence allow for analysis of elemental composition for a wide range of elements simultaneously.

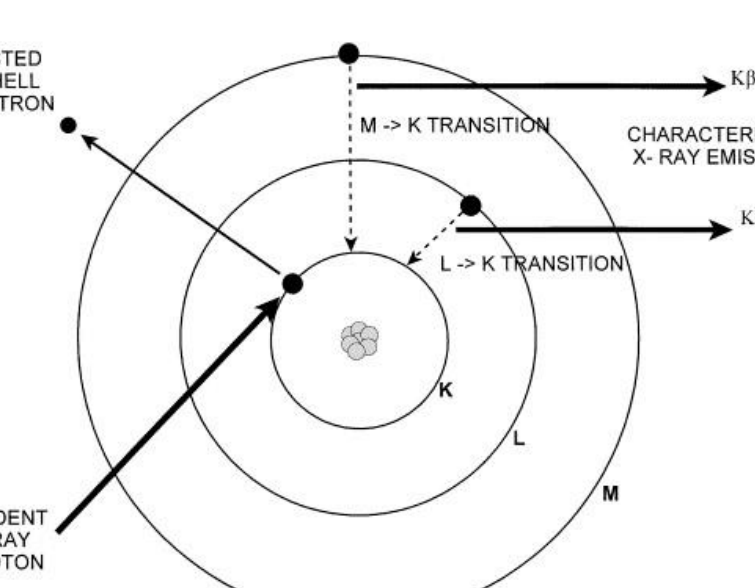
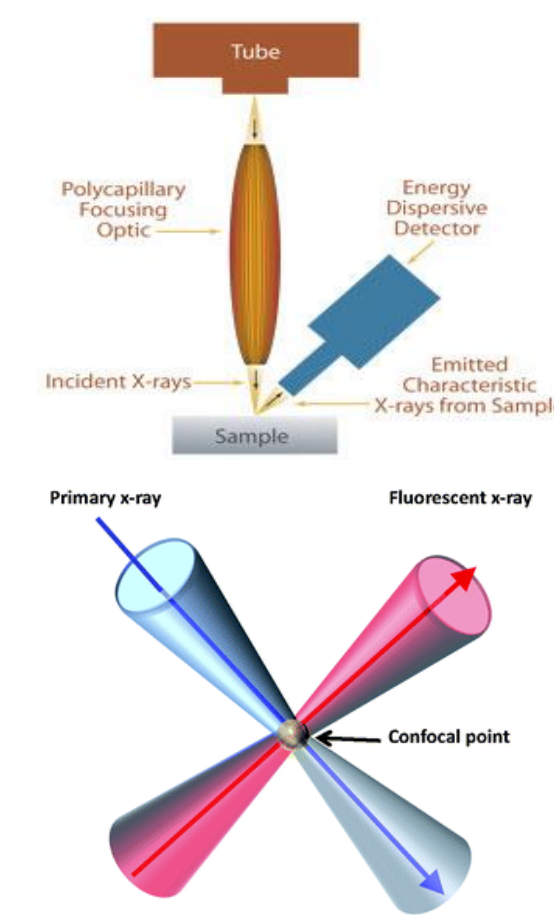


Figure 3: Basic principles of XRF. The K, L and M shells refer to core electron shells.



Micro X-Ray Fluorescence (Micro-XRF)

XRF is measured by the number of x-ray photons detected at these characteristic energies, reporting counts on an energy spectrum. The energy of the fluorescent photon is measured in kilo electron-volts (keV).

In micro-XRF the x-rays are produced by an x-ray tube and focused to a point by the optic. Figure 3 demonstrates one such arrangement. The focal point of the optic and detector coincide so that only the fluorescent x-rays emitted from the confocal point will be detected as illustrated in Figure 4.

Figure 4: (Top) A

Instrument Specifications

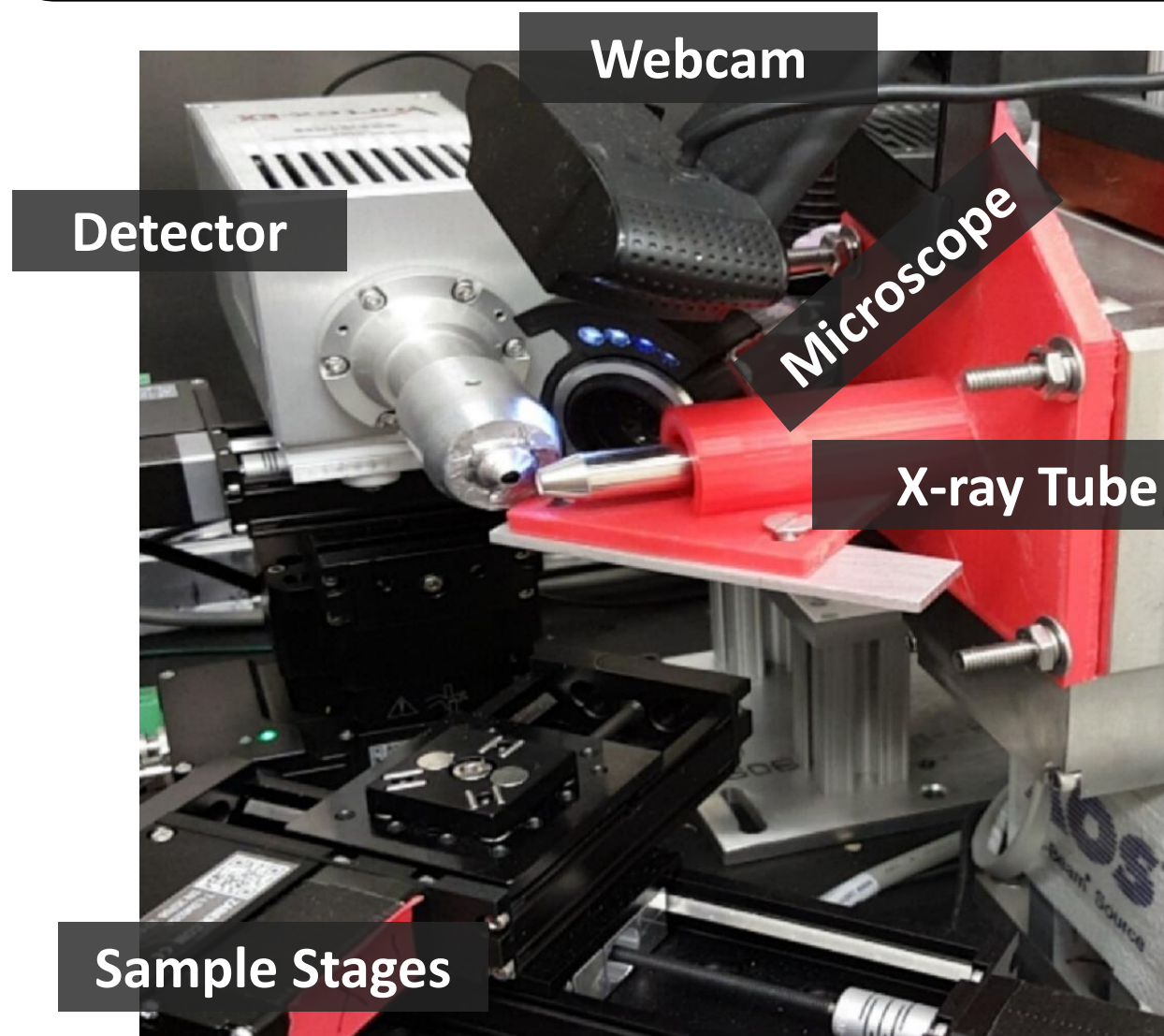


Figure 4: The micro-XRF with component callouts

The experimental micro-XRF used in this study was custom built by the Fittschen group. The geometry of the micro-XRF is designed so that the sample is at a 45 degree angle to the x-ray source and the detector for a 90 degree detection angle. The stages move the sample along x, y and z axes during scanning to create the map. A webcam and 5x magnification microscope focused on the beam focal point is used to visually examine and align the sample while the custom build steel x-ray shielding enclosure is shut.

| Element | Group | Relative Kraft standard | AXO standard | Sensitivity [CPS/(ng/mm ²)] | STD | RSTD % |
|---------|-------|-------------------------|--------------|---|-------|--------|
| S | Ka | 18% | 4.3 | 0.703 | 16.4 | |
| K | Ka | | 9.3 | | | |
| Ca | Ka | 57% | 59% | 11.1 | 0.092 | 0.83 |
| Ti | Ka | 79% | | 14.8 | | |
| V | Ka | 88% | | 16.5 | | |
| Cr | Ka | 98% | | 18.4 | | |
| Mn | Ka | 100% | | 18.7 | | |
| Fe | Ka | 100% | 100% | 18.8 | 0.039 | 0.21 |
| Co | Ka | 93% | | 17.4 | | |
| Ni | Ka | 84% | | 15.8 | | |
| Cu | Ka | 68% | | 12.5 | 0.095 | 0.76 |
| Zn | Ka | 59% | | 11.1 | | |

Table 1: Relative sensitivity for relevant elements as determined from a 13 element Kraft standard solution and AXO free standing reference film.

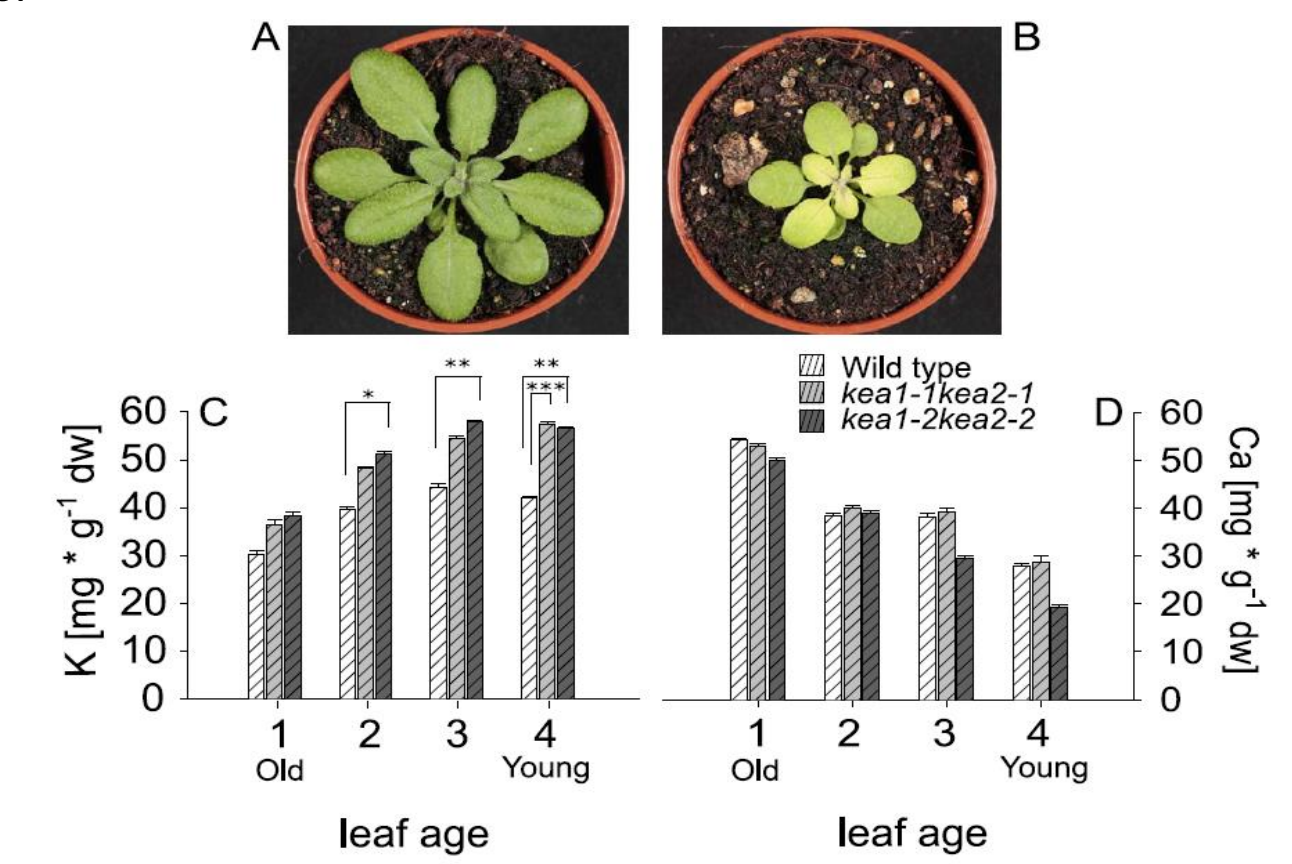
The relative elemental sensitivity of the micro-XRF were determined using a 13 element Kraft standard solution and a AXO free standing reference film (no matrix) reported in Table 1. The sensitivity to K was interpolated from the plot of relative sensitivity vs. energy of the Kraft and AXO standards. Detection limits for Fe and Pb were determined to be comparable to detection limits of second generation synchrotron facilities.

The beam focal point area was determined to be 14 μ m at the Rh Ka line (20.217 keV) and 32 μ m at the Fe K-edge (7.111 keV) determined by knife edge scan.

Ionome analysis

The nature of x-ray fluorescence spectrometry allows for a wide range of elements to be analyzed simultaneously, and the addition of a series of mobile sample stages allows for mapping of elemental concentrations across the surface of the sample. These elemental maps are used for ionome analysis. Ionomics is the study of an organisms' ionome, the total elemental composition of the organism or its parts. Ionome analysis is useful in determining homeostatic distribution of elements in plants for assessing deficiencies of vital macronutrients such as zinc and iron and macronutrients like calcium and magnesium or excesses of nutrients that could be toxic in high concentrations.

This study aims to explore the capability of the custom built micro-XRF for phenotyping by micro-ionome analysis differentiating between plant organs like veins and mesophyll. In previous work, the concentrations of K and Ca were analyzed by Total X-ray Fluorescence (TXRF) at various plant ages to determine the effect that age has on these concentrations for both the mutant and wild type plants [Hoehner et al]. The results presented in Figure 5 found that the plant age did have a significant impact on the observed bulk concentration of K and Ca.



Plant Analysis Methods

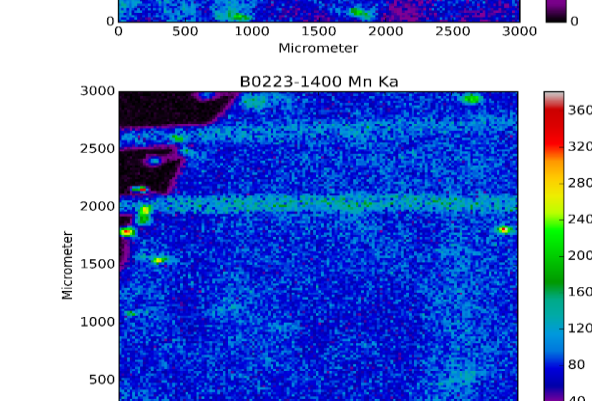
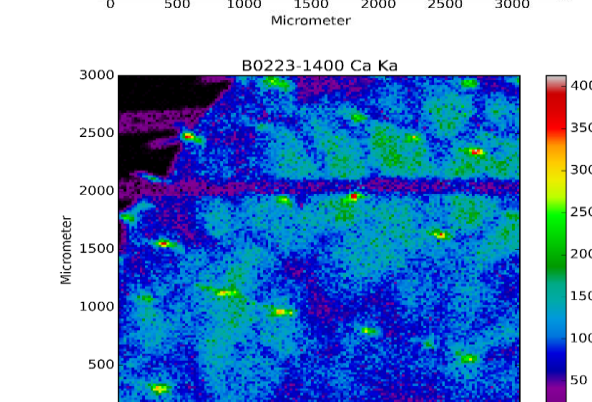
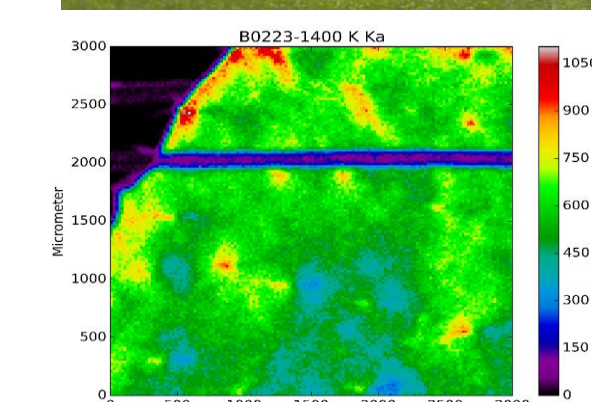
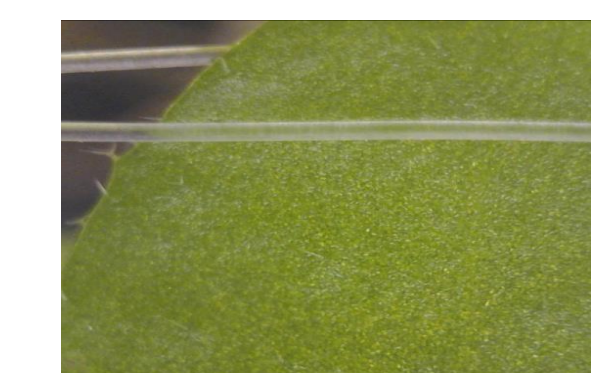


Figure 4: a) Optical image of the leaf b) K spectral map, filament not visible c) Ca spectral map, filament not visible d) Mn spectral map, filament visible behind leaf tissue.

K and Ca concentrations were analyzed as elemental maps produced by scanning of the leaves. The standard analysis parameters were 250-350 ms lifetime per spectra with steps of 20 to 40 μ m. These parameters were used to limit radiation exposure to the plant while still producing sufficient counts for characterization.

Detection limits of a sample measured by the micro-XRF depend on the element in question, since spectral lines and line intensity vary with each element and the background which is determined by the matrix. The sensitivity of a spectral line is affected by the efficiency of excitation, the fluorescence yield and matrix-absorption. Low Z elements fluoresce at lower energies, but lower energy x-rays are more easily absorbed and emitted at more shallow depths within the sample while higher energy x-rays pass deeper into the sample. This effect is defined as the information depth, referring to the depth that information can be retrieved from. This is observed as high concentrations of light elements like K and Ca at the surface, while heavier elements like Fe, Mn, Cu and Zn are observed deeper in the tissue as illustrated in Figure 4. Matrix effects such as absorption by water affect the observed counts, affecting the observed concentrations in the sample especially with low Z elements like K and Ca. These issues of absorption from the water and uncertainty in information depth in the plant cells has to be addressed to ensure that the reported concentrations are meaningful.

To verify the accuracy of the concentrations determined by micro-XRF results were compared with results obtained from TXRF. Circular punches 3 mm in diameter were taken from several leaves. The leaves were desiccated in an oven to eliminate the absorption effects introduced by the water matrix and analyzed by micro-XRF. In an earlier work punches have been digested with nitric acid. The digested samples were analyzed by TXRF to determine analyte concentrations in terms of mg/g of analyte per mass of dried plant matter [Hoehner et al]. Relating the analyte mass to the dried sample mass is important for comparing the concentrations determined by TXRF to those obtained from the in vivo specimens and dry leaves.

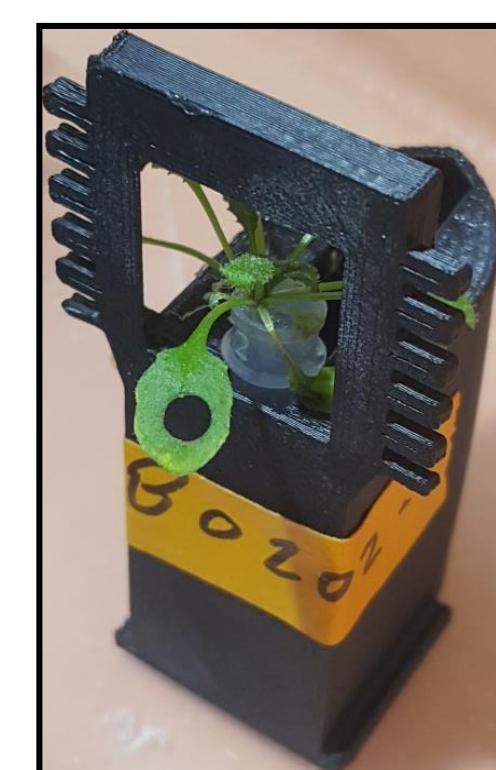


Figure 5: Arabidopsis thaliana plant with a punch removed from the leaf.

Results and Discussion

In vivo measurements

Data was collected for six mutant type plants and four wild type plants. Each mutant plant was scanned once, but scans of the wild type plants were done by two different methods. Of the four wild type plants, two were scanned once and the other two were scanned once as whole leaves then a 3 mm disk was punched from the leaf and dried. The disks were scanned to compare the normalized concentration measured by the micro-XRF with those determined with the TXRF, but these concentrations cannot be compared directly with those determined for the in vivo specimens because of the absorption of the water matrix. Table 2 shows the concentration of K and Ca determined by the in-vivo scans using the free standing film as a reference. As the information depth of K is around 50 μ m and Ca 60 μ m and the leaf thickness varies between 100-200 μ m the results are not representative of the bulk content.

| Mutant | K (ng/mm ²) | Ca (ng/mm ²) |
|------------|-------------------------|--------------------------|
| A1007-1529 | 198 | 54 |
| A1010-1420 | 150 | 159 |
| A1012-1500 | 191 | 38 |
| A1014-1611 | 162 | 31 |
| A1019-1500 | 153 | 38 |
| A1021-1208 | 144 | 73 |
| Average | 166 | 65 |
| St.Dev | 21 | 44 |
| %RSD | 13% | 67% |

| Wild | K (ng/mm ²) | Ca (ng/mm ²) |
|-------------|-------------------------|--------------------------|
| A1024-1330 | 112 | 27 |
| B0117-1400 | 118 | 55 |
| B0202-1500 | 78 | 82 |
| B0223-1400* | 253 | 34 |
| Average | 102 | 54 |
| St.Dev | 18 | 22 |
| %RSD | 17% | 41% |

Table 2:

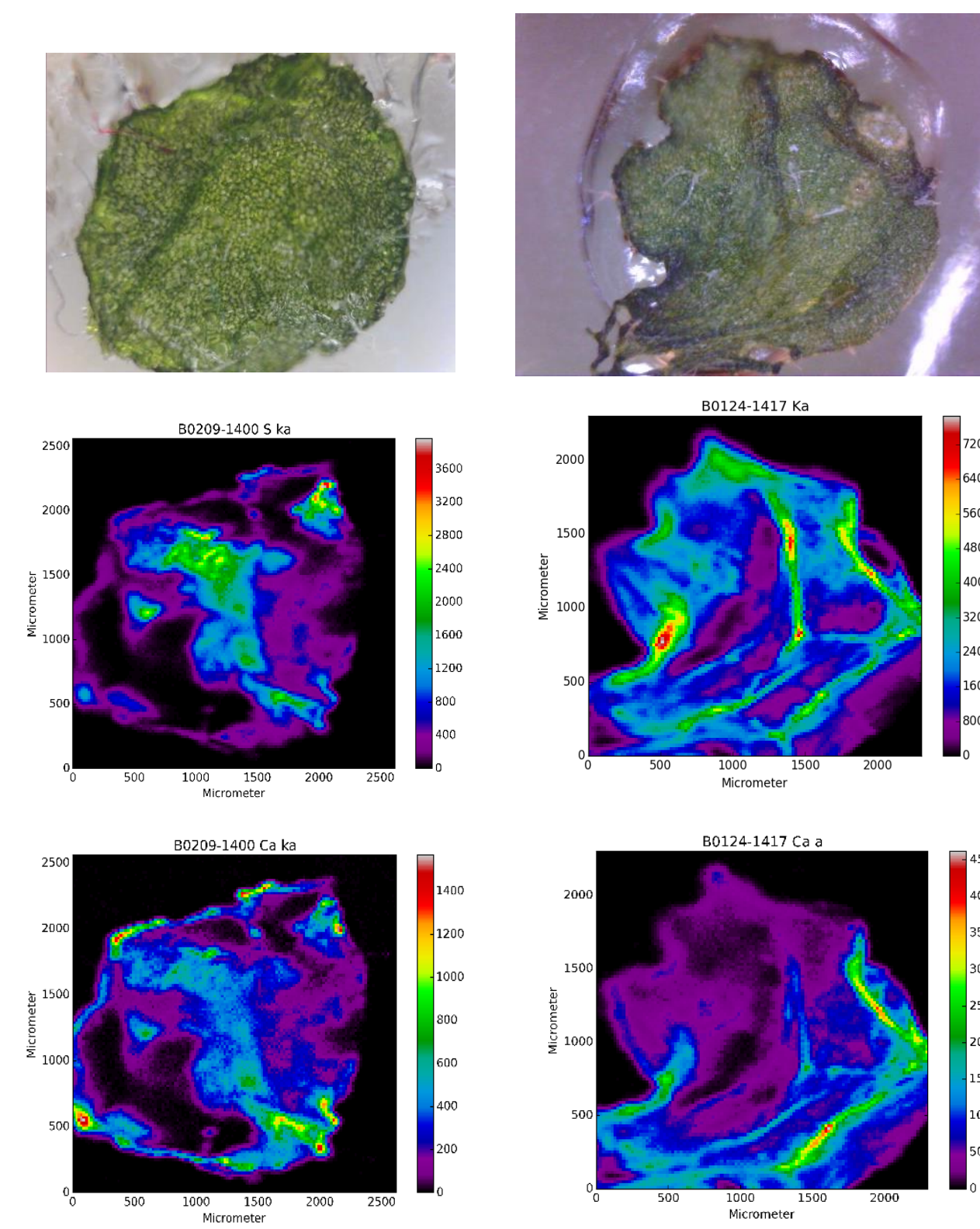
Dried leaf scans

The disks that were punched from the leaves grown on hydroponic media were dried then scanned in order to compare the micro-XRF concentrations to those determined by TXRF for both hydroponically-grown K and Ca concentrations and soil-grown K concentration. The counts per second were normalized over the number of pixels which contained spectral data of the plant matter, then converted to estimated concentrations using the instruments' sensitivity to each element. The mass was converted to concentration in terms of mass element per mass of the dry leaf punch. Since the punch mass varied between 60 and 150 μ g for those used in the TXRF analysis, the upper and lower limits were used to approximate the mass of these punches, giving a concentration range for K and Ca for each punch scanned (Table 3).

While there is not enough data to make a conclusion about the actual concentrations of each element in the sample, the estimated concentrations determined from the data are relatively close to those from the TXRF analysis. It was observed in the composite images that after drying, K distribution was more concentrated inside of the leaf than Ca which tended to be more concentrated around the edges of the punch. This can be seen in Figures 6-8. This does

| Scan label | Element | ng/punch (ng) | Mass per 60ug Punch (ng/mg) | Mass per 150ug Punch (ng/mg) | Concentration range (mg/g) |
|------------|---------|---------------|-----------------------------|------------------------------|----------------------------|
| B0124-1417 | K | 2885 | 48 | 19 | 19-50 |
| | Ca | 934 | 16 | 6 | 6-16 |
| B0209-1200 | K | 904 | 15 | 6 | 6-15 |
| | Ca | 359 | 6 | 2 | 2-6 |
| B0302-1400 | K | 3231 | 54 | 22 | 22-54 |
| | Ca | 147 | 2 | 1 | 1-3 |

| Grow method | Element | Concentration range (mg/g) |
|-------------|---------|----------------------------|
| Soil grown | K | 30-45 |
| Hydro grown | K | 38-58 |
| Hydro grown | Ca | 8-14 |



Discussion

In general, the K concentrations seem to be higher in the mutant than in the wild type. Besides B0223-1400 which has extremely high K concentration for a wild type, however the appearance of the plant indicated that this specimen was not a wild type genotype. In general, the Ca concentration seems to be lower than the K concentration besides sample A1010-1420 and B0202-1500. The B0223-1400 K concentration can be explained by the area that was scanned. Earlier work and literature data has shown that the ion concentration change depending on the scanned tissue, mesophyll, vein or trichome. In A1010-1420 mainly a trichome was scanned which has in general higher Ca concentration than K.

Another possible source of error in this study is environmental stress on the plant. Environmental stress may affect the concentrations faster than the micro-XRF can complete a scan of the leaf. These stressors include elevated temperature inside the enclosure, absence of light during the plants' normal "daylight" hours, and exposure to the x-ray source. This effect could be studied by taking repeated scans of a small leaf section over a time frame of one to two hours to determine whether the observed concentration of a highly mobile element such as Ca changes with respect to the time spent in the enclosure. Care should be taken to ensure that repeated scanning of one section of the leaf does not damage the plant tissue.

The micro-XRF stages are capable of moving the sample in three dimensions, x, y and z, described as depth, horizontal and vertical respectively. Currently a scan can only record spectra while moving through two axes with the third axis fixed. This approach is appropriate for most samples, however the surface of the leaf is not uniform and causes the x-ray beam to move in and out of focus during the scan as the leaf surface depth changes relative to the focal point. It is not known how the change in depth affects the spectra that are recorded when the beam is not aligned with the leaf surface, but this could be studied in more detail with Confocal-micro-XRF. CMXRF records data as the beam spot moves along all three axes, probing the volume element rather than just the surface area.

Conclusion

This study surveyed a small number of plants of wild and mutant phenotype with the intent of determining the phenotype of the plant solely from micro-XRF analysis. A large amount of data was collected on several plants over the course of the study, however not enough data was collected to say with certainty whether the mutant plants exhibited a unique phenotype compared to the wild type plants as demonstrated with TXRF [Hoehner et al].

As more data was collected more sources of uncertainty were discovered over the course of the study that should be considered for future analysis, such as the overall health of the plants between being transferred to the lab and when they were scanned and the impact of the enclosure on the plant health. The limited time frame available for an undergraduate student to collect data only worsened the uncertainty since the plants aged significantly between consecutive scans of the same specimen. A larger more controlled study of several dozen plants of each type that accounted for plant age would likely yield more significant results about the phenotyping of plants using micro-XRF. The concentrations in the leaf punches were relatively close to those determined with

TXRF, but a larger study should be done to determine average values for the wild and mutant type plants using both micro-XRF and TXRF. On the other hand, as a preliminary study of the application of micro-XRF for phenotyping, much was learned regarding methodology as the study progressed. The standardization of growing conditions, living conditions and the analysis process would help to reduce uncertainty in analysis of living samples, and regular sensitivity and intensity evaluation for the x-ray source are necessary for maintaining the quality of analysis.

Future work would likely begin with addressing the issue of information depth for individual elements by upgrading the micro-XRF to a confocal setup. Following this, a larger revised study of the *Arabidopsis thaliana* ionome and phenotyping would be the next priority. Unfortunately, after the conclusion of this study the x-ray intensity dropped significantly, indicating an issue with the x-ray tube. The optic cannot be repaired in the lab and must be returned to XOS for the time being, putting future work on hold until the micro-XRF is returned to working condition.

References

- U. E. A. Fittschen, H.-H. Kunz, R. Höhner, I. M. B. Tyssebotn, A. Fittschen, A new micro X-ray fluorescence spectrometer for in vivo elemental analysis in plants, X-ray Spectrom. (2017) under consideration
- Ricarda Hoehner, Samaneh Tabatabaei, Hans-Henning Kunz, Ursula Fittschen, A rapid total reflection X-ray fluorescence protocol for micro analyses of ion profiles in Arabidopsis thaliana; Spectrochimica Acta Part B: Atomic Spectroscopy (2016) 125, 159-167, doi: 10.1016/j.sab.2016.09.013
- Punshon, T.; Ricachenevsky, F. K.; Hindt, M. N.; Socha, A. L.; Zuber, H., Methodological approaches for using synchrotron X-ray fluorescence (SXRF) imaging as a tool in ionomics: examples from Arabidopsis thaliana. *Metallomics* 2013, 5 (9), 1133-1145.

Salt, D. E.; Baxter, I.; Lahner, B., Ionomics and the Study of the Plant Ionome. *Annual Review of Plant Biology* 2008, 58, 709-733.